Journal of Orthopaedic Translation 36 (2022) 109–119

Contents lists available at ScienceDirect

Journal of Orthopaedic Translation

journal homepage: www.journals.elsevier.com/journal-of-orthopaedic-translation

Evaluation of interbody fusion efficacy and biocompatibility of a polyetheretherketone/calcium silicate/porous tantalum cage in a goat model

Kai Yuan [a,1], Kai Zhang [a,1], Yiqi Yang [a], Yixuan Lin [a], Feng Zhou [a], Jingtian Mei [a], Hanjun Li [a], Jie Wei [b], Zhifeng Yu [a,***], Jie Zhao [a,**], Tingting Tang [a,*]

[a] Shanghai Key Laboratory of Orthopaedic Implants, Department of Orthopaedic Surgery, Shanghai Ninth People's Hospital, Shanghai Jiao Tong University School of Medicine, Shanghai, 200011, China
[b] Key Laboratory for Ultrafine Materials of Ministry of Education, School of Materials Science and Engineering, East China University of Science and Technology, Shanghai, China

ARTICLE INFO

Keywords:
PEEK
Calcium silicate
Porous tantalum
Interbody fusion cage
Biocompatibility
Spine surgery

ABSTRACT

Objective: To evaluate the interbody fusion efficacy and biocompatibility of a graft-free cage made of polyetheretherketone/calcium silicate composite/porous tantalum (PEEK/CS/pTa cage) compared with a PEEK/CS cage with an autogenous bone graft in a goat model.

Methods: PEEK/CS/pTa and PEEK/CS cages were prepared through an injection-moulding method. The PEEK/CS composites and porous tantalum were characterized by Fourier transform infrared spectroscopy (FTIR), X-ray photoelectron spectroscopy (XPS), X-ray diffraction (XRD), scanning electron microscopy (SEM), and energy-dispersive spectroscopy (EDS) mapping. Then, adult goats were chosen for C2/C3 and C3/C4 discectomy via the anterior cervical approach and randomly implanted with PEEK/CS/pTa and PEEK/CS/cages with autogenous bone grafts. The fusion performance and osseointegration of the cages were evaluated by X-ray imaging, magnetic resonance imaging (MRI) scanning, and bone histomorphometry analysis. Moreover, the concentrations of Ca and Si in urine, serum, tissue around the fusion segments and major organs of the goats were determined by inductively coupled plasma–optical emission spectrometry (ICP–OES). Histological observation of major organs of the goats was used to evaluate the biosafety of PEEK/CS/pTa and PEEK/CS cages.

Results: X-ray and MRI imaging suggested that both PEEK/CS/pTa cages and PEEK/CS cages maintained similar average intervertebral space heights. The tissue volumes in the fusion area were comparable between the two groups of cages at 26 weeks after surgery. Histological morphometric data showed that PEEK/CS/pTa cages and PEEK/CS cages with autogenous bone grafts had similar bone contact and osseointegration at 12 and 26 weeks. Element determination of serum, urine, spinal cord, dura matter, bone and organs showed that the CS/PEEK cages did not cause abnormal systemic metabolism or accumulation of calcium and silicon in local tissues and major organs of goats after implantation. No obvious pathological changes were found in the heart, liver, spleen, liver or kidney tissues.

Conclusion: Overall, these results suggested that the graft-free PEEK/CS/pTa cage showed similar bony fusion performance to the PEEK/CS cages with autogenous bone grafts. The cages releasing calcium and silicon had good biological safety in vivo.

The translational potential of this article: This study provided a new graft-free interbody fusion solution to patients with degenerative disc diseases, which could avert potential donor-site complications. This study also

* Corresponding author. Shanghai Key Laboratory of Orthopaedic Implants, Department of Orthopaedic Surgery, Shanghai Ninth People's Hospital, Shanghai Jiao Tong University School of Medicine, Zhizaoju Road 639, Shanghai, 200011, China.
** Corresponding author. Shanghai Key Laboratory of Orthopaedic Implants, Department of Orthopaedic Surgery, Shanghai Ninth People's Hospital, Shanghai Jiao Tong University School of Medicine, Zhizaoju Road 639, Shanghai, 200011, China.
*** Corresponding author.
E-mail addresses: zfyu@outlook.com (Z. Yu), profzhaojie@126.com (J. Zhao), ttt@sjtu.edu.cn (T. Tang).
[1] Kai Yuan and Kai Zhang contributed equally to this work.

https://doi.org/10.1016/j.jot.2022.06.006
Received 24 January 2022; Received in revised form 11 April 2022; Accepted 22 June 2022

provided a detailed assessment of element excretion and accumulation of Ca and Si in vivo, which validated the biosafety of this new type of bioactive interbody fusion cage.

1. Introduction

Discectomy and fusion are effective surgical procedures to treat degenerative disk diseases and rebuild spinal stability. Most surgeons apply interbody fusion cages to enhance spinal mechanical endurance and augment spine function [1]. Autogenous bone grafts are usually packed with interbody fusion cages and act as osteogenesis substrates to achieve bony fusion in the long term [2]. For decades, autogenous bone grafts have been widely regarded as the gold standard for interbody fusion due to their strong osteogenic potential and complete histocompatibility [3–5]. However, the acquisition of autogenous bone grafts inevitably causes trauma in the donor site and could potentially lead to multiple kinds of donor-site complications, such as persistent donor-site pain, deep haematoma formation, deep infection, incisional hernia, and donor-site fracture [6,7]. According to previous reports, 2%–37.9% of patients suffered donor-site pain 6 months after the operation, and 2.5% of patients suffered deep infection at the donor site [8–11]. The limited bone availability and donor-site complications drove the development of alternative materials [12–14].

Porous tantalum, recognized as an effective material for artificial metal trabecular bone, has been used in spine surgery for years [15–17]. Porous tantalum has a high volumetric porosity, which allows ingrowth of nearby tissue and subsequent osteogenesis [18]. In addition, the Young's modulus of porous tantalum was approximately 3–4 GPa, which was relatively similar to that of cancellous bone (approximately 10.4 GPa) [19] and could avert the stress-shielding effect of traditional metal implants [18,20]. In addition, porous tantalum has strong corrosion–resistant properties and good biocompatibility [18,21,22]. In previous studies, porous tantalum has been proven to show considerably good osteoconductive and osteoinductive performance in a cervical interbody model, with evident trabecular bone ingrowth and osseointegration at the fusion interface [23]. Therefore, porous tantalum is an ideal alternative material to autogenous bone grafts.

Among the various kinds of materials used for interbody cages, polyetheretherketone (PEEK) accounts for a large percentage because of its good biocompatibility and moderate elastic modulus, similar to cancellous bone [24–26]. PEEK cages were biologically inert, and this property led to relatively high biosafety as well as some disadvantages, including fibrous healing and low osseointegration at the implant surface [27]. With the efforts of recent years, various methods have been developed to improve the biological activity of PEEK, such as surface coatings made of titanium or hydroxyapatite and other incorporated composites [28–31]. In our previous studies, we designed and developed a compounding and injection-moulding technique to incorporate calcium silicate (CS) into PEEK to manufacture a PEEK/CS composite material, which was optimized for osteogenesis with a CS ratio of 40% by weight (wt%) [32,33]. A comparative study showed that the PEEK/CS interbody fusion cage had a better pro-osteogenic effect in vitro and better fusion and osseointegration performances in vivo than the pure PEEK interbody fusion cage in a goat cervical interbody fusion model [34]. Based on these findings, we step further to replace the packed-in autogenous bone graft with porous tantalum and designed a new PEEK/CS/pTa cage that could potentially avert trauma and complications at the donor site and achieve similar fusion performance and osseointegration. This study was designed to compare the interbody fusion performance of PEEK/CS/pTa cages and PEEK/CS cages packed with autogenous bone grafts and investigate the calcium (Ca) and silicon (Si) distribution in the body, with the aim of laying a foundation for biosafety assessment and clinical translation.

2. Materials and methods

2.1. Preparation of interbody fusion cage

The PEEK/CS composite interbody fusion cage was manufactured as previously described. In brief, PEEK powder (Solvay Specialty Polymers, GA, USA) and micron-sized calcium silicate powders were blended in a ball mill (QM-3B, T-Bota Ltd., China) with a weight ratio of 6/4 for 1 h. Then, the mixed powders were dried at 150 °C for 24 h and heated to 380 °C in an injection-moulding machine (BA-300/050CD, Awans, Belgium) and fabricated into PEEK/CS composites, which were further processed through a turning lathe (C616-1, Jinan First Machine Tool Group Co. Ltd., China) and cut into interbody fusion cage rings. For PEEK/CS/pTa interbody fusion cage preparation, the inner void space of the PEEK/CS interbody fusion cage was filled with a pre-cut porous tantalum metal block (Trabecular MetalTM VBR-21, Zimmer Biomet, USA) with a size of 5 mm × 5 mm × 3 mm. Otherwise, the inner void space was filled with the autogenous bone graft, which was harvested from the iliac crest during the operation. The specific shape and size of these interbody fusion cages are shown in Fig. 1.

2.2. Characterization of PEEK/CS/pTa interbody fusion cage

The surface morphology, element composition and distribution of the PEEK/CS interbody fusion cage and porous tantalum metal block were characterized by field-emission scanning electron microscopy (SEM, S4800, HITACHI, Japan) and energy-dispersive spectrometry (EDS, S4800, HITACHI, Japan). The composition of the PEEK/CS interbody fusion cage was determined by X-ray photoelectron spectroscopy (XPS, ESCALAB 250, Thermo Scientific, USA) and Fourier transform infrared spectroscopy (FTIR, Nicolet iN10, Thermo Scientific, USA), and the phase structure of the porous tantalum metal block was determined by X-ray diffraction (XRD, Rigaku Ultima IV, Rigaku Corporation, Japan).

2.3. Animal model and surgical procedures

An anterior cervical discectomy and fusion model in goats was carried out according to our previous study [34]. All animal procedures and experiments were reviewed and approved by the Animal Ethical Committee of Shanghai Ninth People's Hospital. The approval number is SH9H-2021-A649-1. In brief, 15 female goats (2 years old, 40–50 kg) were purchased from Shanghai Jiagan Biotechnology Company and accustomed to the new environment for one week before the surgery. The PEEK/CS cages and PEEK/CS/pTa cages used for surgery were sterilized by ethylene oxide sterilization. On the day of surgery, the goats were anaesthetized with gas anaesthesia (isoflurane) and fixed on the operation table in a supine position with tracheal intubation inserted to maintain an unobstructed airway. Then, the skin of the neck area was disinfected with an iodophor and 75% ethanol scrub. After this, a longitudinal skin incision was made 1.5 cm to the left of the midline of the neck. Then, we fully exposed the operation field of the ventral C2/C3 and C3/C4 disc surfaces for discectomy, which made enough intervertebral space for interbody cage implantation. The PEEK/CS and PEEK/CS/pTa interbody fusion cages were randomly implanted in the intervertebral space of C2/C3 and C3/C4 in a goat. The inner holes of the PEEK/CS interbody fusion cage were filled with autogenous bone grafts harvested from the iliac crest. Additionally, a titanium plate was utilized to fix the cervical vertebrae. Finally, routine closure was performed, and 4 million

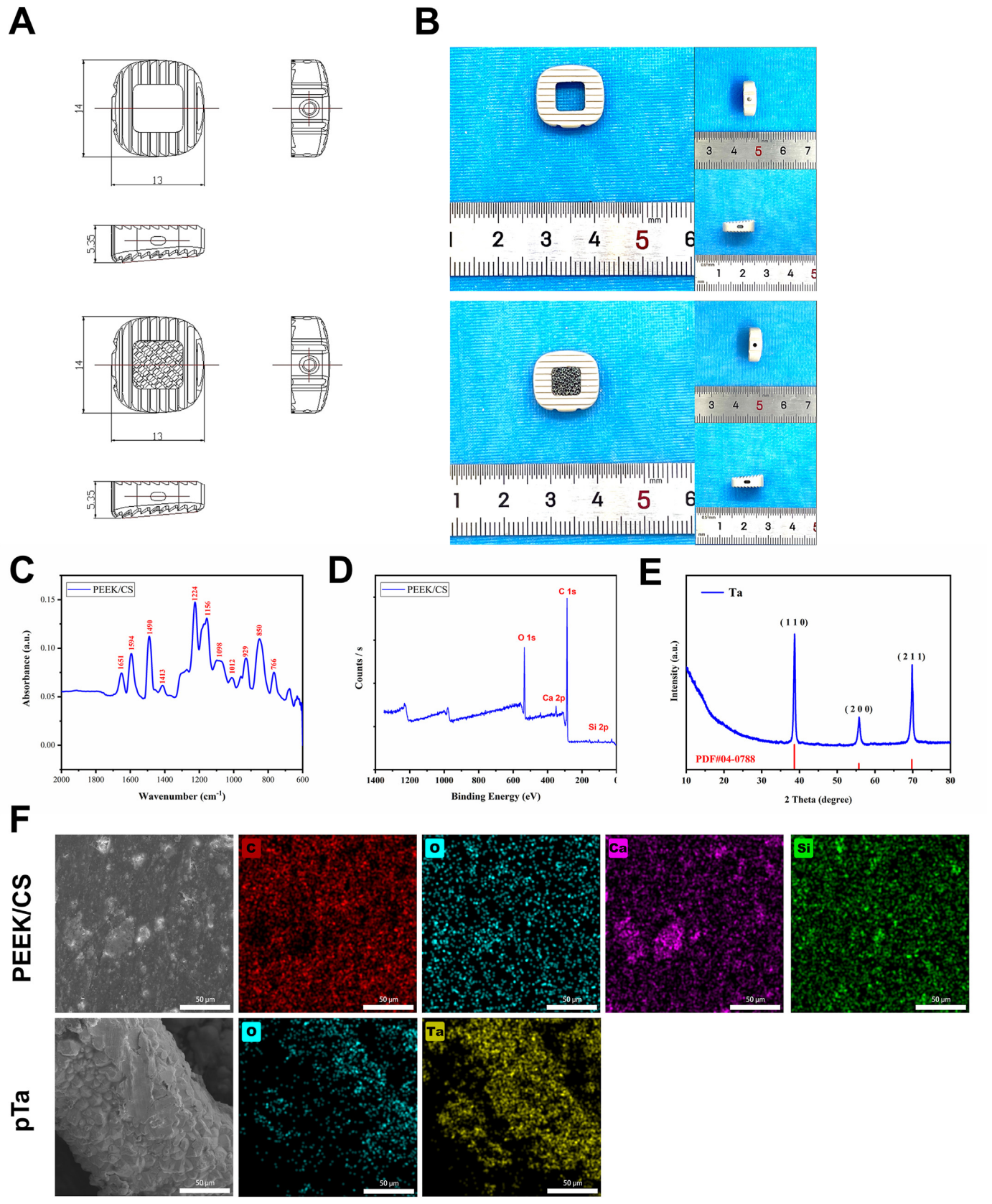

Fig. 1. Design and characterization of PEEK/CS and PEEK/CS/pTa interbody fusion cages. (A) Schematic design of the PEEK/CS (upper) and PEEK/CS/pTa (lower) interbody fusion cages. (B) Photographs of the actual PEEK/CS (upper) and PEEK/CS/pTa (lower) interbody fusion cages. (C) FTIR spectra of the PEEK/CS composites. (D) Full XPS spectra of the PEEK/CS composites. (E) XRD pattern of the porous tantalum scaffold. (F) SEM images and EDS mapping of the PEEK/CS composites and porous tantalum scaffold.

units of penicillin sodium were intramuscularly injected into each goat for 5 days after surgery. Goats that had undergone surgery were carefully raised and monitored for any adverse reactions and complications until they reached corresponding endpoints. Goats were intramuscularly injected with alizarin red solution (20 mg/kg) and calcein solution (20 mg/kg) 2 weeks and 3 days before being sacrificed. As indicated in Fig. 2A, at each endpoint, goats were euthanized, and the main organ tissues, including heart, liver, spleen, lung, kidney, and cervical spinal segments, were immediately collected. Some of the main organ tissues were immersed in 4% formalin solution, and the remaining organ tissues and spinal segments were stored at −20 °C for further analysis.

2.4. X-ray analysis

At predetermined time points (Fig. 2A), goats were anaesthetized, and lateral cervical X-ray images were harvested with an X-ray DR system (Ultimax, TOSHIBA, Japan). The average interbody disc space height (DSH) was determined to evaluate the fusion performance as previously described. Briefly, the average DSH was measured from the lateral cervical X-ray images according to the following formula: The average DSH = (anterior DSH + middle DSH + posterior DSH)/3 [34,35].

2.5. Magnetic resonance imaging (MRI) scanning and analysis

A high-field MRI scanning system (BRUKER BIOSPEC 70/30 MRI, BRUKER BIOSPEC, Germany) was used to detect and analyse the tissue formation and fusion performance of interbody cages. In brief, experimental spinal segments were sawed to a proper length. After this, the samples were subjected to a high-field MRI scan with a field strength of 7 T and a slice thickness of 0.5 mm. The tissue volume was selected with a global threshold in the inner space of the interbody fusion cage in T1-weighted imaging; the signals were further reconstructed to 3D images and used to quantify the tissue volume. MRI data analysis and reconstruction were performed with 3D Slicer software (Version 4.11).

2.6. Undecalcified bone histomorphometry

Experimental spinal segment samples at two time points were subjected to undecalcified bone histomorphometry analysis to determine the bone formation rate in the fusion area and bone-implant contact as previously reported [34]. In brief, spinal segment samples were dehydrated in a graded ethanol series. The samples were then embedded in methyl methacrylate (MMA, Merck, Schuchardt, Germany) monomer for 2 weeks. After this, the samples were transferred into an embedded device with colloidal MMA and stored at room temperature until the embedded samples totally solidified. Then, the solidified samples were cut into thin 100 μm slices using a microtome (SP1600, Leica, Germany). The slices were fixed on plastic slides and polished to approximately 50 μm, and Van Gieson staining was performed according to the manufacturer's instructions. Finally, the volume of new bone in the fusion area was measured with Image-Pro Plus 6.0 software (Media Cybernetics, United States). Three sections of each sample were randomly chosen for analysis.

2.7. Fluorescence microscopy analysis

Dynamic bone formation during the observation period was tracked by double labelling with alizarin red and calcein, which have already been widely applied in labelling bone tissue. Image-Pro Plus 6.0 software was used to measure the bone formation rate and bone-implant contact

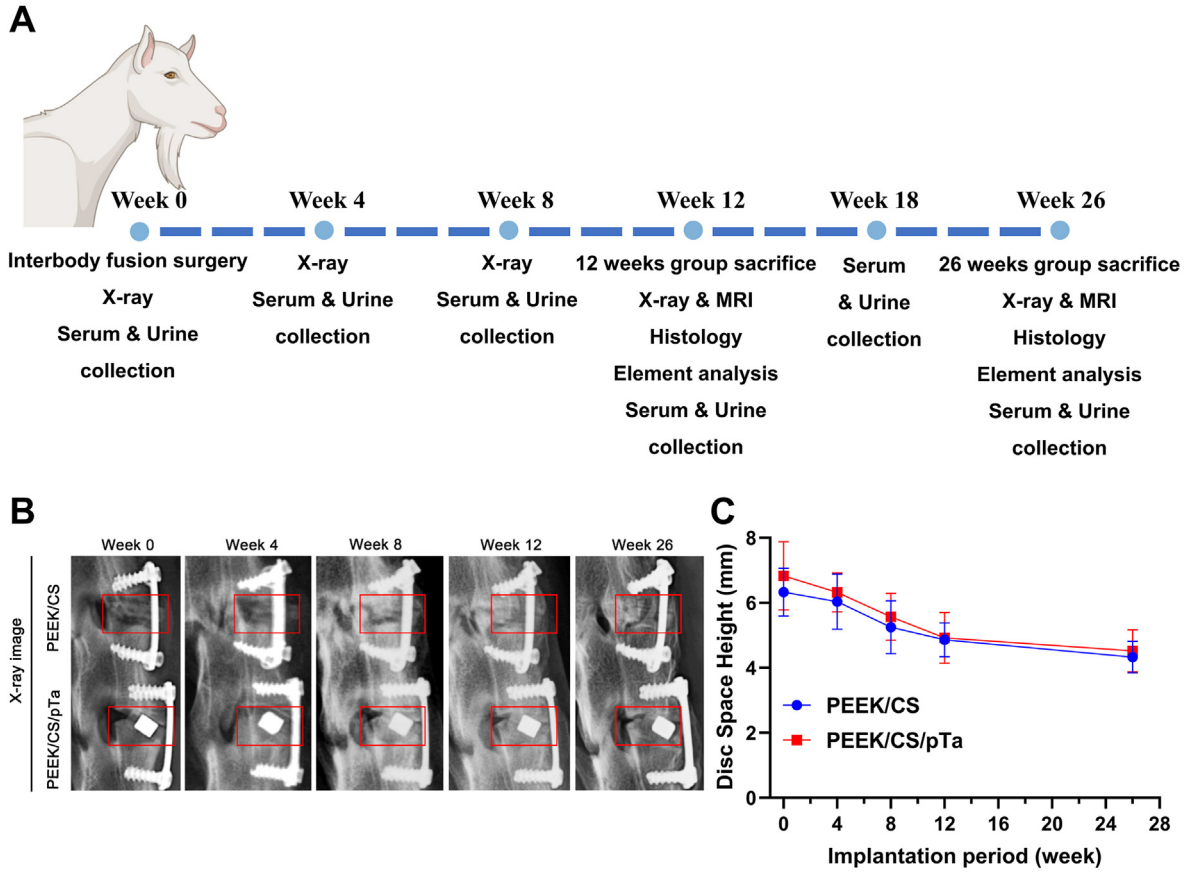

Fig. 2. Experimental design of the goat interbody fusion model and DSH analysis based on X-ray radiography. (A) Schematic illustration of the surgery and analysis procedures of the goat interbody fusion model. (B) Representative X-ray images at 0, 4, 8, 12, and 26 weeks. (C) DSH analysis at 0 (n = 15), 4 (n = 15), 12 (n = 15), and 26 weeks (n = 8).

rate by observing the fluorescence labelling on slides with confocal laser scanning microscopy (CLSM, Leica, Germany).

2.8. Analysis of elemental Ca and Si

The metabolism of calcium and silicon released from PEEK/CS and PEEK/CS/pTa cages was monitored by determining the concentrations of Ca and Si in the serum and urine of the goats before and after the operation. The accumulation of Ca and Si in goats' major organs, including the heart, liver, spleen, lung, and kidney, was determined and compared with that of normal healthy female goats. The element concentrations of Ca and Si in bone, dura mater, and spinal cord from operation segments and distal segments (C7) were also measured and compared. Serum and urine samples from goats were collected at 0, 4, 8, 12, 18, and 26 weeks after the operation, and major organ samples of goats and cervical spine segments were harvested immediately after goats were sacrificed. All samples were stored at −80 °C until being analysed. The samples were digested with aqua regia supplemented with 0.25% hydrofluoric acid for 1 h at 180 °C using a microwave digester (ultraWAVE, Milestone, USA) and further analysed for Ca and Si concentrations by inductively coupled plasma optical emission spectroscopy (ICP–OES, Agilent 720 ES, Agilent, USA). To prevent potential Si contamination during sample processing, urine samples were collected with catheters made of polyvinyl chloride (PVC), and all serum and urine samples were stored in polypropylene tubes and chemically digested in Teflon vessels [36,37].

2.9. Histological analysis of major organs

After the goats were sacrificed at predetermined time points, the major organs, including the heart, liver, spleen, lung, and kidney, were collected from goats. Some organ tissues were separated and fixed in 4% paraformaldehyde. The specimens were then embedded in paraffin embedding and cut into 4 μm slices. The changes in the histology of major organs were observed by microscopy with H&E staining.

2.10. Statistical analysis

In this experiment, all data were analysed with SPSS 13.0 software (Statistical Package for the Social Sciences, USA) and presented as the means ± standard deviation. We used two-way analysis of variance (two-way ANOVA) to analyse the data of average interbody disc space height. Multigroup parametric data of element concentrations of Si and Ca in urine, serum, major organs, bone, dura mater, spinal cord and degradation rate of PEEK/CS interbody fusion cage were compared with one-way analysis of variance (ANOVA) followed by Tukey's test. The tissue formation data determined by MRI, bone-implant contact rate, and bone volume in the fusion area were analysed with the t test.

3. Results

3.1. Characterization of PEEK/CS/pTa interbody fusion cage

The design draft and actual products of PEEK/CS and PEEK/CS/pTa cages are shown in Fig. 1A–B. FTIR analysis (Fig. 1C) of the PEEK/CS composites showed the characteristic peaks of PEEK. XPS analysis (Fig. 1D) of the PEEK/CS composites revealed the surface composition of calcium silicate. The surface element of tantalum was validated by the signal dots of tantalum of the EDS mapping (Fig. 1F) and characteristic peaks of tantalum in the XRD result (Fig. 1D). SEM and EDS spectrum images (Fig. 1F) demonstrated the rough surface of PEEK/CS composites and porous tantalum scaffolds. The signal dots of Ca and Si had a relatively even distribution pattern on the surface of PEEK/CS composites.

3.2. X-ray imaging and DSH measurement

To monitor interbody fusion, X-ray photographs were performed at predetermined time points (Fig. 2A). As shown in Fig. 2B, in both fusion segments of PEEK/CS cages with autogenous bone grafts and PEEK/CS/pTa cages, an increased density of upper and lower endplates and high-density bony ingrowth were observed at 12 weeks. At 26 weeks, bridging bone was formed between the fusion segments of PEEK/CS cages with autogenous bone grafts. Quantitative measurement (Fig. 2C) revealed that DSH in segments of PEEK/CS cages with autogenous bone grafts or those with PEEK/CS/pTa cages gradually decreased during the follow-up period from 0 to 12 weeks, and no significant difference was observed between the two groups, which indicated that PEEK/CS/pTa cages had fusion stability similar to that of PEEK/CS cages with autogenous bone grafts.

3.3. MRI scanning and analysis

To quantify and visualize the tissue ingrowth and 3D structure in the fusion segments, MRI scanning and tissue volume analysis were performed. As shown in Fig. 3A, obvious tissue ingrowth and bridging tissue formation were observed in both fusion segments of PEEK/CS with autogenous bone grafts and PEEK/CS/pTa cages at 12 weeks and 26 weeks. Quantitative analysis of tissue volume revealed that PEEK/CS cages with autogenous bone grafts supported a higher volume of new tissue growth than PEEK/CS/pTa cages at 12 weeks ($p < 0.01$). The tissue volume in the fusion area of PEEK/CS cages with autogenous bone grafts remained slightly higher than that of PEEK/CS/pTa cages at 26 weeks. However, no obvious significant difference was found between these two groups, which indicated that both the PEEK/CS/pTa and PEEK/CS cages with autogenous bone grafts had satisfactory fusion performance.

3.4. Osseointegration assessment by histomorphometry analysis

Undecalcified bone histomorphometry analysis served as the gold standard for assessing osseointegration and bony fusion. To evaluate the osseointegration performance of PEEK/CS cages with autogenous bone grafts and PEEK/CS/pTa cages, newly formed bone around the cage was double-labelled with fluorescence. As shown in Fig. 4A, fluorescence-labelled mineralized bone was found at the contact surfaces of both cages at 12 weeks. At 26 weeks, denser fluorescence labelling was found at the contact surfaces of both cages. Bone-implant contact analysis (Fig. 4B) revealed that osseointegration of PEEK/CS cages with autogenous bone grafts increased from 33.99 ± 6.57% (12 weeks) to 62.29 ± 6.47% (26 weeks), while the bone-implant contact ratio at the contact interface of PEEK/CS/pTa increased from 31.75 ± 5.20% (12 weeks) to 62.27 ± 13.69% (26 weeks). There were no significant differences between the two groups at either time point. As shown in Fig. 4C, bone tissue formed in the fusion area inside the cages was stained with Van Gieson staining. At 12 weeks, continuously mineralized bone ingrowth was found in PEEK/CS cages with autogenous bone grafts, and deposition of newly formed bone was observed in the porous tantalum scaffolds of PEEK/CS/pTa cages. At 26 weeks, continuously mineralized bone tissue was observed in both PEEK/CS cages with autogenous bone grafts and PEEK/CS/pTa cages. Bone volume in the fusion area was quantitatively analysed, as shown in Fig. 4D, which indicated that PEEK/CS cages with autogenous bone grafts supported more mature mineralized bone tissue formation than PEEK/CS/pTa cages at 12 weeks ($p < 0.05$) and 26 weeks ($p < 0.01$).

3.5. Determination of Ca and Si levels in serum and urine

To monitor the levels of elemental Ca and Si in the serum and urine of goats, serum and urine samples were collected before and after surgery at predetermined time points and were further analysed by ICP–OES. As shown in Fig. 5A, the Ca concentration in the urine of goats showed a

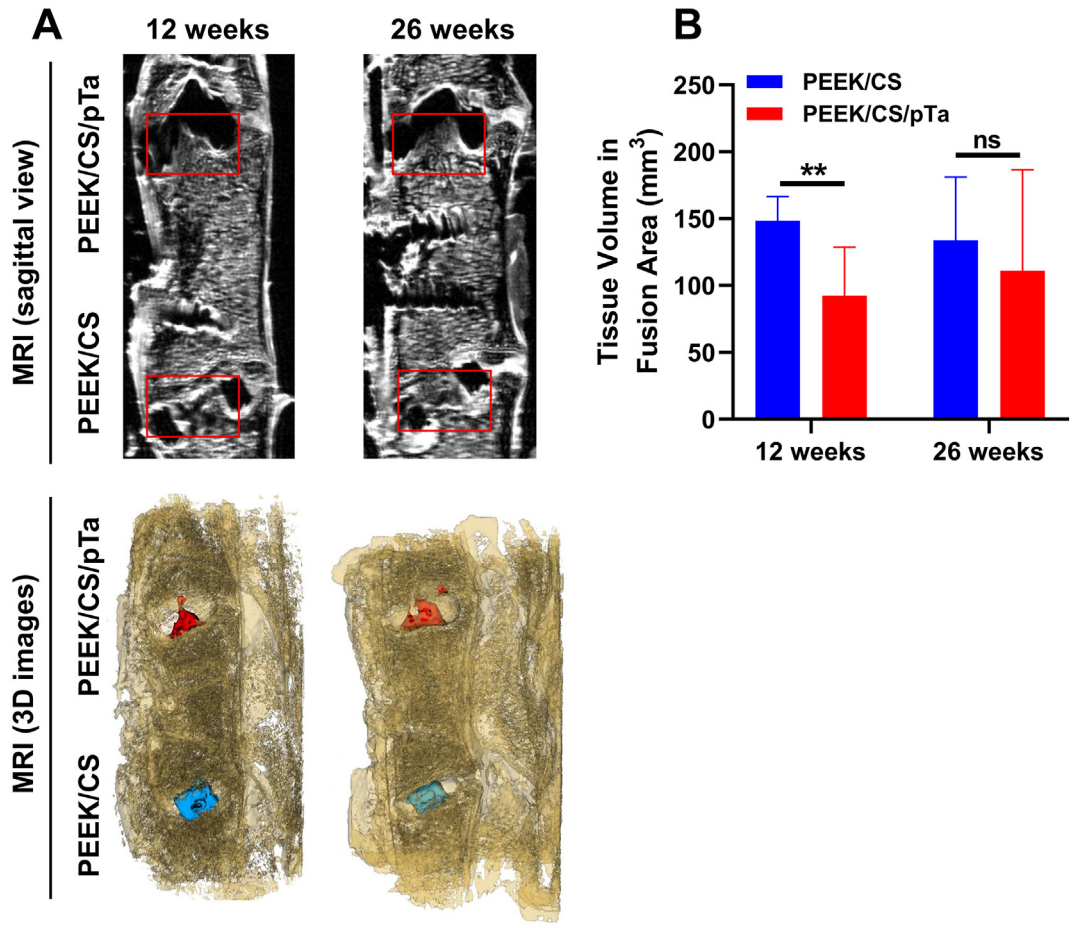

Fig. 3. MRI scanning and analysis of tissue formation in the fusion area. (A) Representative sagittal images of MRI scanning and 3D reconstructed MRI images. (B) Analysis of tissue volume in the fusion area of the PEEK/CS cage and PEEK/CS/pTa cage at 12 weeks (n = 7) and 26 weeks (n = 8). ** indicates $p < 0.01$ for comparison between the two groups; ns indicates no significant difference was found between the two groups.

relatively steady pattern during the whole observation period. The Ca concentration in the serum of goats (Fig. 5B) remained relatively steady at 0, 4, and 8 weeks but showed a significant decrease at 12 weeks and subsequently rose to normal levels (0 weeks) at 18 and 26 weeks. For Si concentration in the urine of goats, Fig. 5C demonstrates that there was no difference in Si level in urine during the observation period except for 26 weeks, at which time it was significantly increased compared with 0 weeks. Si concentration in serum (Fig. 5D) at 8 and 18 weeks significantly decreased compared with 0 weeks, while no difference in the serum Si concentration was observed at 4, 12, or 26 weeks compared with 0 weeks.

3.6. Determination of Ca and Si levels in tissues

To detect the accumulation of Ca and Si in major organs, the heart, liver, spleen, lungs and kidneys were collected and subjected to element analysis. The results showed that the Ca content in the liver and kidneys of surgically manipulated goats was not different from that of normal goats (Fig. 6B and E). The Ca contents in the liver, spleen, and lungs of surgically manipulated goats at 12 weeks were significantly lower than those of normal goats (Fig. 6A, C, 6D). However, these differences diminished at 26 weeks. At 12 and 26 weeks, the Si content in the heart, liver, spleen, lungs, and kidneys of surgically manipulated goats showed no difference compared with those of normal goats (Fig. 6G–J). These results demonstrated that no obvious Ca or Si accumulation was found in surgically manipulated goats implanted with cages made of PEEK/CS composite. Although the Ca content in some organs (heart, spleen, and lung) of surgical goats was lower than that of normal goats, this transient fluctuation was restored to normal levels at 26 weeks. Element analysis of Ca and Si in local tissues, including the spinal cord, dura mater, vertebral bone at the fusion segments and distal segments and new bone formed at the fusion segments, was also carried out to determine the element deposition in tissues around the interbody fusion cages. Compared with distal segments, there was no difference in Ca and Si content in the spinal cord and dura mater of fusion segments (Fig. S1A-B, D-E). In terms of bone tissues, the results (Fig. S1F) of Si content in vertebral bone showed no difference among distal segments, fusion segments and new bone at 12 weeks and 26 weeks. The Ca content in new bone was significantly higher than that of vertebral bone of fusion segments at 12 weeks and 26 weeks (Fig. S1C). The overall results implied that Ca and Si content in tissues was maintained at a normal level.

3.7. Histological observation of major organs

Histological sections and H&E staining of major organs of goats were performed to determine whether pathological changes existed in goats implanted with cages. As shown in Fig. 7, in all goats at 12 weeks and 26 weeks, no obvious histologic abnormalities were observed, indicating that PEEK/CS and PEEK/CS/pTa cages and their degradation products are non-toxic to the major organs of goats.

4. Discussion

Recent years have witnessed the rapid development of artificial and synthetic graft materials, including ceramics, porous metals, polymers, bioactive glass, demineralized bone matrix (DBM) and other composite

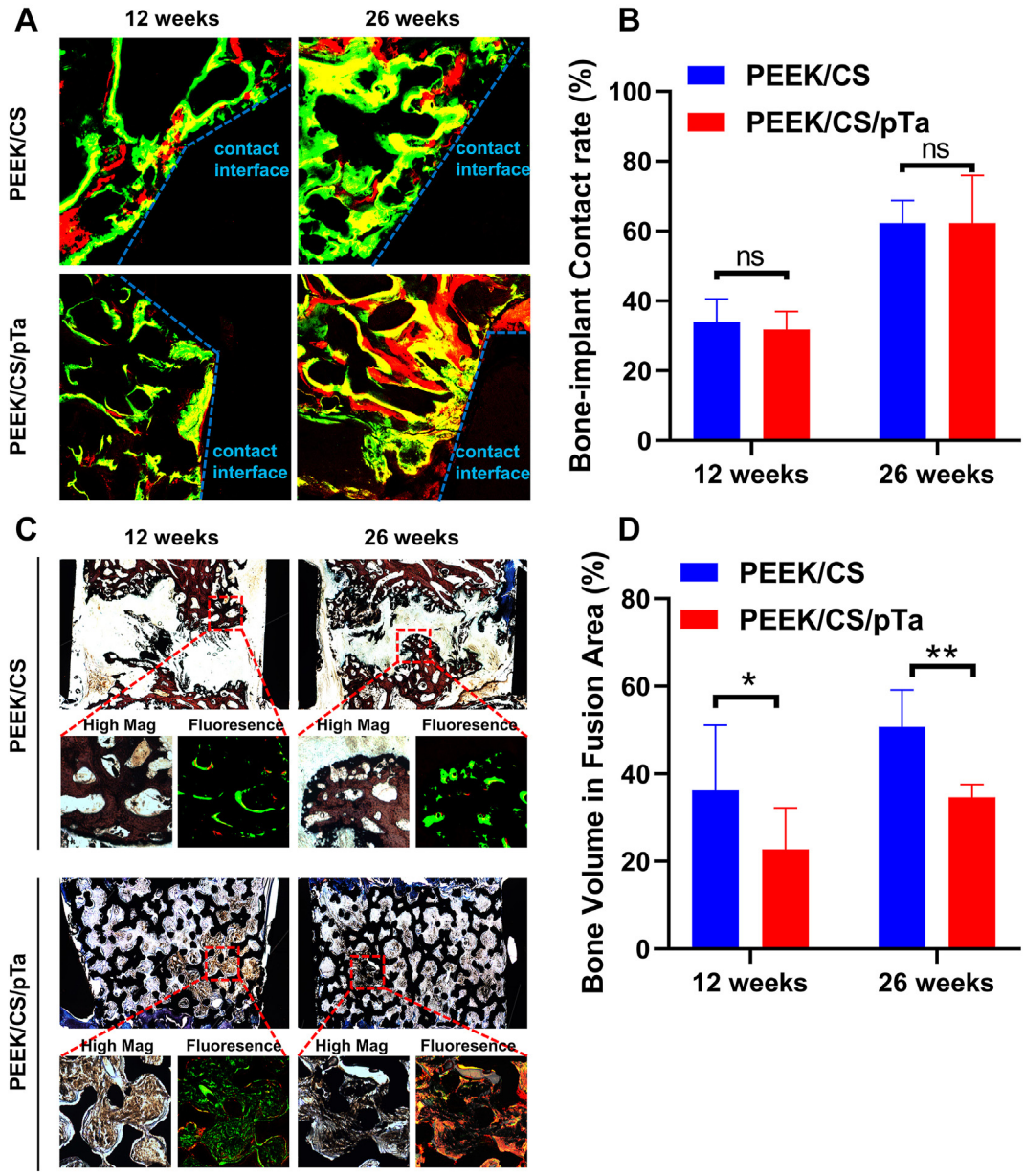

Fig. 4. Analysis of osseointegration and bone formation at 12 and 26 weeks based on undecalcified histological assessment. (A) Osseointegration labelled with calcein and alizarin red at the contact surface of the bone implant. (B) Quantitative comparison of the bone implant contact rate of PEEK/CS and PEEK/CS/pTa cages at 12 weeks (n = 7) and 26 weeks (n = 8). (C) Overall view and high magnification images of Van Gieson staining and fluorescence images of high magnification view labelled with calcein and alizarin red in the fusion area. (D) Quantitative comparison of bone formation in the fusion area of PEEK/CS and PEEK/CS/pTa cages at 12 weeks (n = 7) and 26 weeks (n = 8). * and ** indicate $p < 0.05$ and $p < 0.01$ for comparison between the two groups, respectively; ns indicates no significant difference was found between the two groups.

materials consisting of pro-osteogenic factors [38–41]. Unlike degradable materials such as ceramic material, bioactive glass and DBM, porous tantalum scaffolds serve as permanent implants, exhibiting strong mechanical properties and enabling a rapid postoperative return to movement and exercise [16,42].

Interbody fusion cages made of porous tantalum have been applied in clinical practice for years; however, porous tantalum alone has some limitations in application. Due to the relatively high brittleness [43,44], plastic deformation and cracking of porous tantalum easily occur during the knocking process of the implant surgery, which ultimately reduces the mechanical stability of fusion segments. In most cases of porous tantalum cage implantation, autogenous bone grafts were also used [45, 46]. This study demonstrated that the PEEK/CS cage combined with porous tantalum can serve as a new graft-free interbody fusion cage, which is expected to diminish the donor-site complications of autogenous bone grafts.

To examine whether PEEK/CS/pTa cages could achieve fusion performances similar to those of PEEK/CS cages with autogenous bone grafts, two cages were randomly implanted and fixed in segments of C2/C3 and C3/C4 within a goat. Restoration of DSH after implanting an interbody fusion cage was one of the main goals of interbody fusion. According to the DSH measurement results, there was no significant difference between the DSH of the PEEK/CS/pTa cages and PEEK/CS cages with autogenous bone grafts at 4, 8, 12, and 26 weeks, which reflected the similar fusion stability of these two cages.

Owing to the radiopacity, micro-CT and X-ray cannot show the structure of new bone inside the porous tantalum. According to previous reports, however, artefacts from tantalum metal can be avoided in MRI

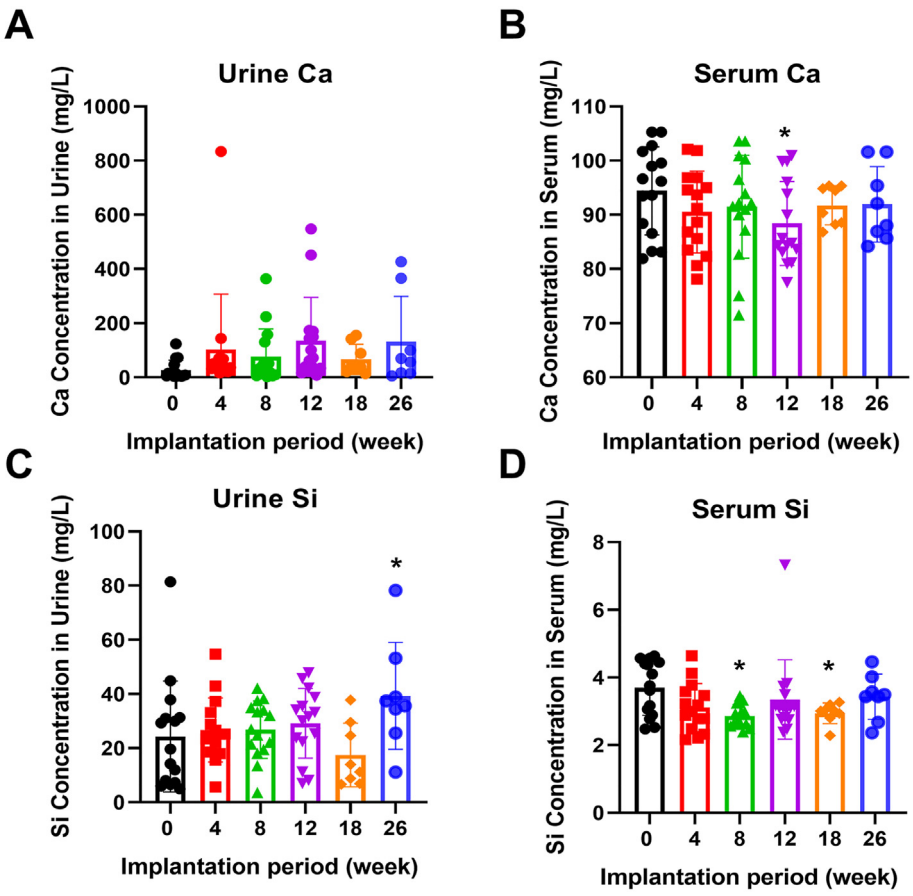

Fig. 5. Analysis of element levels of Ca and Si in urine and serum of the goats. (A–B) Ca concentrations in urine and serum at 0 (n = 15), 4 (n = 15), 8 (n = 15), 12 (n = 15), 18 (n = 8) and 26 weeks (n = 8). (C–D) Si concentrations in urine and serum at 0 (n = 15), 4 (n = 15), 8 (n = 15), 12 (n = 15), 18 (n = 8) and 26 weeks (n = 8). * indicates $p < 0.05$ compared with the 0 weeks.

scanning. Zhou et al. utilized MRI scanning to evaluate the fusion progress of porous tantalum interbody fusion devices in a porcine spinal arthrodesis model and proved that T1-weighted spin-echo MRI scanning was an effective and non-invasive way of assessing spinal interbody fusion with porous tantalum devices [23]. MRI scanning was also reported to be compatible with PEEK devices in vivo [47]. Therefore, in this study, we used high-field T1-weighted spin-echo MRI scanning and 3D reconstruction of MRI images to evaluate the tissue formation and fusion performances of the cages. The MRI results showed that both PEEK/CS/pTa cages and PEEK/CS cages with autogenous bone grafts formed continuous bridging tissue at 12 weeks and 26 weeks. Although the newly formed tissue volume of PEEK/CS/pTa was lower than that of PEEK/CS cages with autogenous bone grafts, there was no significant difference between the tissue volume of these two cages at 26 weeks.

Although the tissue formation assessed by MRI scanning revealed that the tissue volume formed in the fusion area was similar between PEEK/CS/pTa cages and PEEK/CS cages with autogenous bone grafts, the bone volume formed in these two cages was unclear. To investigate bone tissue formation, we utilized undecalcified bone sections and Van Gieson staining to determine the bone volume at the fusion area. The results indicated that the bone volume formed in the fusion area of PEEK/CS cages with autogenous bone grafts was significantly higher than that of PEEK/CS/pTa cages at 12 weeks and 26 weeks. In fact, the existence of porous tantalum took up much space in the fusion area, which may partly account for the lower bone tissue formation inside the PEEK/CS/pTa cages. However, bridging bone tissue was found in both cages at 12 weeks and 26 weeks, which indicated that PEEK/CS/pTa cages could be an alternative to PEEK/CS cages with autogenous bone grafts. Other studies focusing on the osteogenic performance of pTa also confirmed bone ingrowth and occupation of new bone within porous tantalum scaffolds [48,49].

The results of the bone-implant contact rate reflect the osseointegration performance of the cages. Mineralized new bone labelled with calcein and alizarin red was observed at the interfaces between the cages and the ingrowing bone. The bone contact rate of these two cages was similar at 12 weeks and 26 weeks, with no significant difference being found. Porous tantalum exhibits satisfactory osteoconductivity and mechanical properties due to its highly porous structure and lack of osteoinductive inorganic mineral ions and proteins when compared with ceramic and DBM graft materials. Our previous studies demonstrated that PEEK/CS composites facilitated osteogenic differentiation through continuous surface decomposition of PEEK/CS composites and the release of Ca^{2+} and Si^{4+} in the microenvironment, which could facilitate osteoblastic differentiation and osseointegration [32,33]. Ca^{2+} and Si^{4+} supplements from the PEEK/CS composites, to some extent, are expected to improve the osteogenic performance of porous tantalum.

Evaluation of biocompatibility is a crucial step for clinical translation of any new medical device [50–52]. Ca is widely involved in various biochemical reactions and life activities, and the concentration of Ca in blood is precisely maintained in a narrow range to ensure the normal processes of life [53]. As for silicon, an appropriate rate of silicon release contributes greatly to bone repair [54–56]. On the other hand, dysfunction of silicon excretion and abnormal accumulation in organs would lead to structural damage and dysfunction of important organs and death [57,58]. For interbody fusion cages made of PEEK/CS composites, detailed analysis of the metabolism of Ca and Si in vivo is needed to validate their biosafety. In this regard, we continuously monitored the element levels of Ca and Si in the serum and urine of goats before and

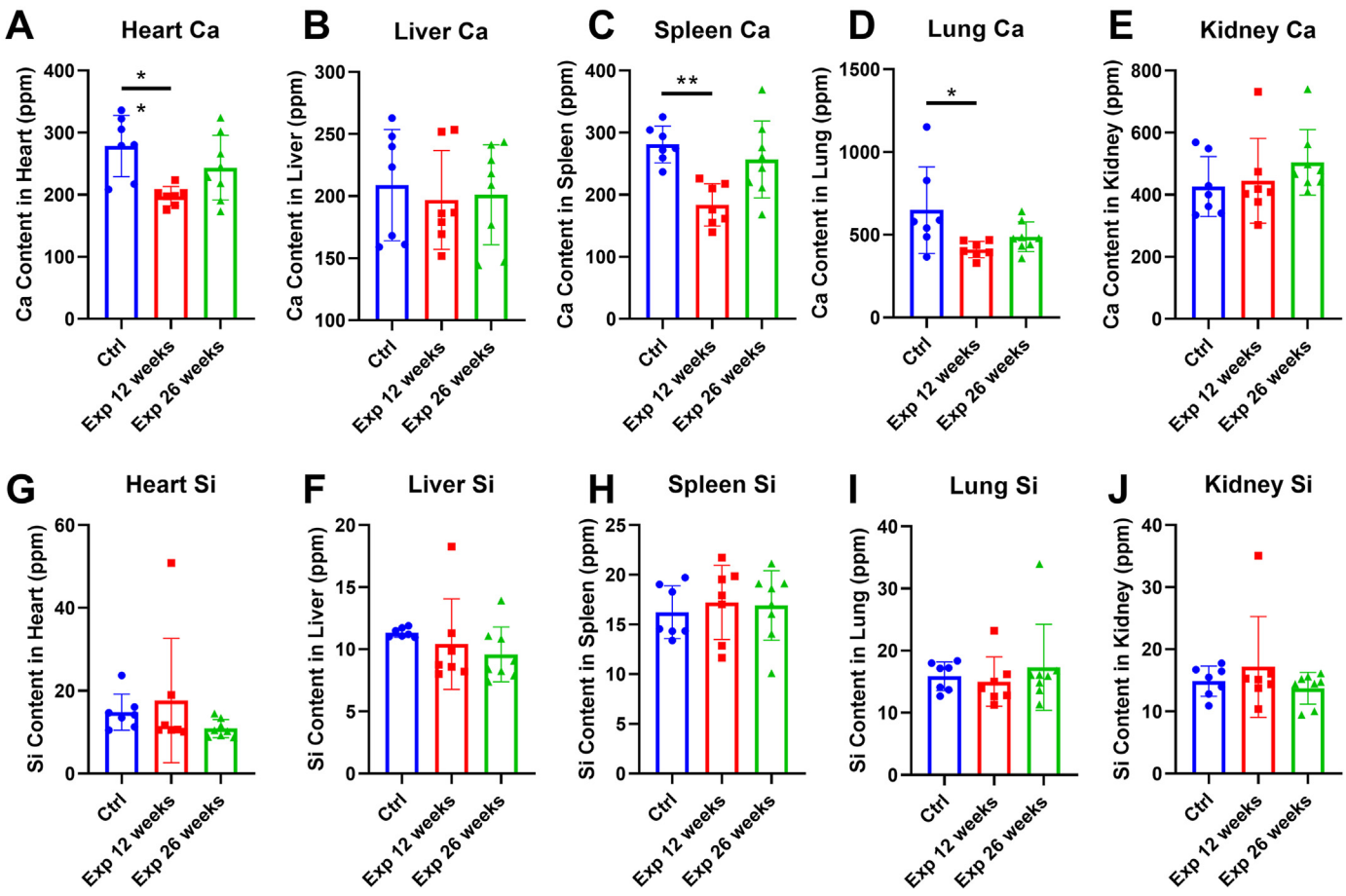

Fig. 6. Analysis of element contents of Ca and Si in major organs of experimental goats (12-week group, n = 7; 26-week group, n = 8) and normal goats (Ctrl group, n = 7). (A–E) Quantitative analysis of Ca content in the heart, liver, spleen, lung and kidney. (F–J) Quantitative analysis of Si content in the heart, liver, spleen, lung and kidney. * and ** indicate $p < 0.05$ and $p < 0.01$ compared with the control group, respectively.

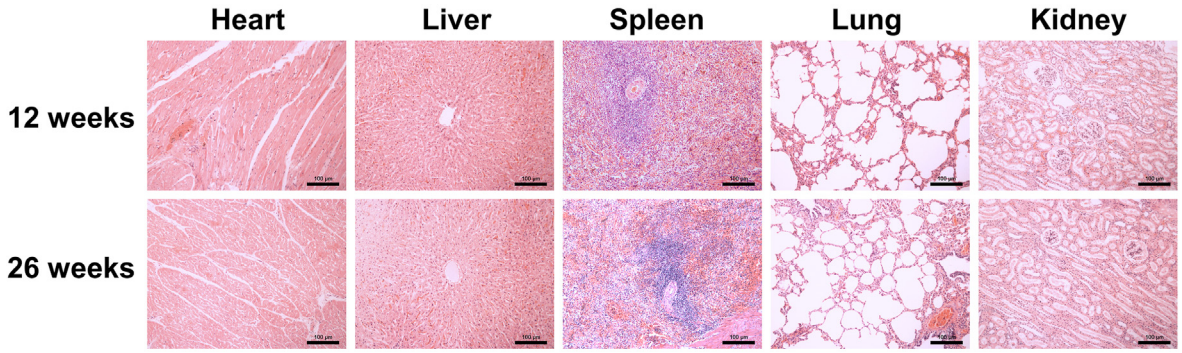

Fig. 7. Histological observation of major organs of experimental goats with cage implantation.

after surgery. The results of element concentrations of Ca and Si in serum and urine demonstrated that the overall element levels of Ca and Si maintained a steady state. The decreased Si content in serum at 8 and 18 weeks and decreased Ca content at 18 weeks may be attributed to increased demands of Ca and Si in tissue repair from 8 to 18 weeks postoperatively, during which bone formation was active. The concentration of Si in urine increased at 26 weeks, which may be associated with decreased demand for Si in the fusion area after active bone regeneration. The level of Si in urine ranges from 3.56 to 81.41 mg/L (ppm), which is far less than the saturation level (180 ppm) of Si in urine [59]. Previous studies on Si excretion from implants demonstrated that Si was constantly dissolved in the circulating interstitial fluid at the implant site and further diffused into the blood, and Si in the blood was mainly excreted in the form of soluble silicate by the kidney [59–61]. In particular, implants placed in bony sites exhibited a slower dissolution rate of Si than implants placed in soft tissue such as muscle [59,60]. The excretion rate of Si by the kidney was estimated to far exceed the dissolution rate of Si at the implant sites, which enables the maintenance of normal levels of Si in the body and avoids the abnormal accumulation of Si in organs [59].

Element content in goat tissues was also measured to examine whether abnormal element deposition and structural damage occurred. The results showed no obvious deposition of Ca or Si in the spinal cord, dura mater, or vertebral bone around the fusion segments except in the newly formed bone. In major organs of goats, including the heart, liver, spleen, lung, and kidney, there was no obvious accumulation of Ca and

Si. We noticed that the calcium content in the heart, spleen, and lung of goats at 12 weeks was lower than that of normal goats. However, this phenomenon was restored to normal at 26 weeks. We assumed that this temporary decrease was associated with increased calcium mobilization and demands in bone regeneration in the fusion area of goats.

Histological observation of major organs of goats further validated the biosafety and biocompatibility of cage implantation. No obvious structural dysfunction or damage was found in the major organs of goats at 12 weeks and 26 weeks after surgery. Several experiments have validated that Si dissolved from bioactive glass and ceramics containing calcium silicate does not cause abnormal accumulation of Si, structural damage or dysfunction in major organs [54,59–61]. The results of Ca and Si levels in this experiment also exhibited overall steady metabolism of Ca and Si in goats implanted with interbody fusion cages made of PEEK/CS composites. All the data lay a strong foundation for the clinical translation of bioactive cages made of PEEK/CS composites in spine surgery.

5. Conclusion

Overall, this study indicated that both PEEK/CS/pTa cages and PEEK/CS cages with autogenous bone grafts supported bone ingrowth and osseointegration in the fusion area and obtained stable fusion performance. Application of PEEK/CS/pTa could potentially avoid autogenous bone graft harvest and donor-site complications, while achieving similar fusion efficacy compared with PEEK/CS cages with autogeous bone graft. The results of element metabolism of Ca and Si in vivo, as well as histological observation of major organs, proved that the PEEK/CS/pTa cage and PEEK/CS cages had credible biosafety and biocompatibility.

Author contributions

Conception and study design: Tingting Tang, Jie Zhao, Zhifeng Yu, Jie Wei, Kai Yuan. Data acquisition and analysis: Kai Yuan, Kai Zhang, Yiqi Yang, Yixuan Lin, Feng Zhou, Jingtian Mei, Hanjun Li. Drafting the manuscript: Kai Yuan and Kai Zhang. Critical revision of the manuscript for intellectual content: Tingting Tang, Jie Zhao, and Zhifeng Yu. All authors agreed to this submission. Kai Yuan and Kai Zhang contributed equally to this study.

Declaration of competing interest

The authors report no conflicts of interest related to this work.

Acknowledgements

This study was supported by the National Key Research and Development Program of China (2016YFC1102102) and the Shanghai Science and Technology Development Fund (19140900104).

Appendix A. Supplementary data

Supplementary data to this article can be found online at https://doi.org/10.1016/j.jot.2022.06.006.

References

[1] Hirvonen T, et al. Anterior cervical discectomy and fusion in young adults leads to favorable outcome in long-term follow-up. Spine J 2020;20(7):1073–84.
[2] Chong E, et al. The design evolution of interbody cages in anterior cervical discectomy and fusion: a systematic review. BMC Muscoskel Disord 2015;16(1):99.
[3] Smith KA, et al. Scientific, clinical, regulatory, and economic aspects of choosing bone graft/biological options in spine surgery. Neurosurgery 2019;84(4):827–35.
[4] Chau AM, et al. Current status of bone graft options for anterior interbody fusion of the cervical and lumbar spine. Neurosurg Rev 2014;37(1):23–37.
[5] Finkemeier CG. Bone-grafting and bone-graft substitutes. J Bone Joint Surg Am 2002;84(3):454–64.
[6] Myeroff C, Archdeacon M. Autogenous bone graft: donor sites and techniques. J Bone Joint Surg Am 2011;93(23):2227–36.
[7] Nassr A, et al. Donor-site complications of autogenous nonvascularized fibula strut graft harvest for anterior cervical corpectomy and fusion surgery: experience with 163 consecutive cases. Spine J 2009;9(11):893–8.
[8] Younger EM, Chapman MW. Morbidity at bone graft donor sites. J Orthop Trauma 1989;3(3):192–5.
[9] Schnee CL, et al. Analysis of harvest morbidity and radiographic outcome using autograft for anterior cervical fusion. Spine (Phila Pa 1976 1997;22(19):2222–7.
[10] Sawin PD, Traynelis VC, Menezes AH. A comparative analysis of fusion rates and donor-site morbidity for autogeneic rib and iliac crest bone grafts in posterior cervical fusions. J Neurosurg 1998;88(2):255–65.
[11] Summers BN, Eisenstein SM. Donor site pain from the ilium. A complication of lumbar spine fusion. J Bone Joint Surg Br 1989;71(4):677–80.
[12] Zhang M, et al. Recent developments in biomaterials for long-bone segmental defect reconstruction: a narrative overview. J Orthop Translat 2020;22:26–33.
[13] Shi GS, et al. Bioactive PLGA/tricalcium phosphate scaffolds incorporating phytomolecule icaritin developed for calvarial defect repair in rat model. J Orthop Translat 2020;24:112–20.
[14] Fu Z, et al. An overview of polyester/hydroxyapatite composites for bone tissue repairing. J Orthop Translat 2021;28:118–30.
[15] Guyer RD, et al. Evaluating osseointegration into a deeply porous titanium scaffold: a biomechanical comparison with PEEK and allograft. Spine (Phila Pa 1976 2016;41(19):E1146–e1150.
[16] Levine BR, et al. Experimental and clinical performance of porous tantalum in orthopedic surgery. Biomaterials 2006;27(27):4671–81.
[17] Fernández-Fairen M, et al. Is anterior cervical fusion with a porous tantalum implant a cost-effective method to treat cervical disc disease with radiculopathy? Spine (Phila Pa 1976 2012;37(20):1734–41.
[18] Liu Y, et al. The physicochemical/biological properties of porous tantalum and the potential surface modification techniques to improve its clinical application in dental implantology. Mater Sci Eng C Mater Biol Appl 2015;49:323–9.
[19] Rho JY, Ashman RB, Turner CH. Young's modulus of trabecular and cortical bone material: ultrasonic and microtensile measurements. J Biomech 1993;26(2):111–9.
[20] Zhao G, et al. Porous tantalum scaffold fabricated by gel casting based on 3D printing and electrolysis. Mater Lett 2019;239:5–8.
[21] Park C, et al. Enhanced endothelial cell activity induced by incorporation of nano-thick tantalum layer in artificial vascular grafts. Appl Surf Sci 2020;508.
[22] Jang T-S, et al. Ta ion implanted nanoridge-platform for enhanced vascular responses. Biomaterials; 2019. p. 223.
[23] Z Z, et al. In vivo magnetic resonance imaging evaluation of porous tantalum interbody fusion devices in a porcine spinal arthrodesis model. Spine 2015;40(19):1471–8.
[24] Kurtz SM, Devine JN. PEEK biomaterials in trauma, orthopedic, and spinal implants. Biomaterials 2007;28(32):4845–69.
[25] Kersten RF, et al. Polyetheretherketone (PEEK) cages in cervical applications: a systematic review. Spine J 2015;15(6):1446–60.
[26] Ahmed AF, et al. The outcomes of stand alone polyetheretherketone cages in anterior cervical discectomy and fusion. Int Orthop 2021;45(1):173–80.
[27] Toth JM, et al. Polyetheretherketone as a biomaterial for spinal applications. Biomaterials 2006;27(3):324–34.
[28] Hasegawa T, et al. The titanium-coated PEEK cage maintains better bone fusion with the endplate than the PEEK cage 6 Months after plif surgery: a multicenter, prospective, randomized study. Spine 2020;45(15).
[29] Lee JH, et al. Cold-spray coating of hydroxyapatite on a three-dimensional polyetheretherketone implant and its biocompatibility evaluated by in vitro and in vivo minipig model. J Biomed Mater Res B Appl Biomater 2017;105(3):647–57.
[30] Buck E, Li H, Cerruti M. Surface modification strategies to improve the osseointegration of poly(etheretherketone) and its composites. Macromol Biosci 2020;20(2):e1900271.
[31] Ma R, Tang T. Current strategies to improve the bioactivity of PEEK. Int J Mol Sci 2014;15(4):5426–45.
[32] Ma R, et al. Preparation, characterization, in vitro bioactivity, and cellular responses to a polyetheretherketone bioactive composite containing nanocalcium silicate for bone repair. ACS Appl Mater Interfaces 2014;6(15):12214–25.
[33] Ma R, et al. Osseointegration of nanohydroxyapatite- or nanocalcium silicate-incorporated polyetheretherketone bioactive composites in vivo. Int J Nanomed 2016;11:6023–33.
[34] Chu L, et al. Highly effective bone fusion induced by the interbody cage made of calcium silicate/polyetheretherketone in a goat model. ACS Biomater Sci Eng 2019;5(5):2409–16.
[35] Cao L, et al. Bioabsorbable self-retaining PLA/nano-sized β-TCP cervical spine interbody fusion cage in goat models: an in vivo study. Int J Nanomed 2017;12:7197–205.
[36] Lin K, et al. Degradation and silicon excretion of the calcium silicate bioactive ceramics during bone regeneration using rabbit femur defect model. J Mater Sci Mater Med 2015;26(6):197.
[37] Fleischer H, et al. Determination of calcium and phosphor in bones using microwave digestion and ICP-MS: comparison of manual and automated methods using ICP-MS. 5th IMEKO TC19 Symposium on Environmental Instrumentation and Measurements 2014; 2014. p. 94–9.
[38] Štoković N, et al. Evaluation of synthetic ceramics as compression resistant matrix to promote osteogenesis of autologous blood coagulum containing recombinant human bone morphogenetic protein 6 in rabbit posterolateral lumbar fusion model. Bone 2020;140:115544.

[39] Westerlund LE, Borden M. Clinical experience with the use of a spherical bioactive glass putty for cervical and lumbar interbody fusion. J Spine Surg 2020;6(1):49–61.
[40] Hyun S-J, et al. A prospective, multi-center, double-blind, randomized study to evaluate the efficacy and safety of the synthetic bone graft material DBM gel with rhBMP-2 versus DBM gel used during the TLIF procedure in patients with lumbar disc disease. J Kor Neurosurg Soc 2021;64(4):562–74.
[41] Plantz M, Gerlach E, Hsu W. Synthetic bone graft materials in spine fusion: current evidence and future trends. Int J Spine Surg 2021;15:104–12.
[42] Zhang Y, et al. Interfacial frictional behavior: cancellous bone, cortical bone, and a novel porous tantalum biomaterial. J Muscoskel Res 1999:245–51. 03(04).
[43] Du Y, et al. Finite element analysis of mechanical behavior, permeability of irregular porous scaffolds and lattice-based porous scaffolds. Mater Res Express 2019;6(10).
[44] Gao HR, et al. Porous tantalum scaffolds: fabrication, structure, properties, and orthopedic applications. Mater Des 2021;210:29.
[45] Zou X, et al. Pedicle screw fixation enhances anterior lumbar interbody fusion with porous tantalum cages: an experimental study in pigs. Spine (Phila Pa 1976 2005; 30(14):E392–9.
[46] Zou X, et al. Bone ingrowth characteristics of porous tantalum and carbon fiber interbody devices: an experimental study in pigs. Spine J 2004;4(1):99–105.
[47] Meng X, et al. A partial hemi-resurfacing preliminary study of a novel magnetic resonance imaging compatible polyetheretherketone mini-prosthesis for focal osteochondral defects. J Orthop Translat 2021;26:67–73.
[48] Bobyn JD, et al. Characteristics of bone ingrowth and interface mechanics of a new porous tantalum biomaterial. J Bone Joint Surg Br 1999;81(5):907–14.
[49] Bobyn JD, et al. Tissue response to porous tantalum acetabular cups: a canine model. J Arthroplasty 1999;14(3):347–54.
[50] Bernard M, et al. Biocompatibility of polymer-based biomaterials and medical devices - regulations, in vitro screening and risk-management. Biomater Sci 2018; 6(8):2025–53.
[51] Lecocq M, et al. Biocompatibility of four common orthopedic biomaterials following neuroelectromyostimulation: an in-vivo study. J Biomed Mater Res B Appl Biomater 2018;106(3):1156–64.
[52] Song W, et al. In vivo biocompatibility and bioactivity of calcium silicate-based bioceramics in endodontics. Front Bioeng Biotechnol 2020;8:580954.
[53] Goff JP. Calcium and magnesium disorders. Vet Clin North Am Food Anim Pract 2014;30(2):359–81. vi.
[54] Wang C, et al. The enhancement of bone regeneration by a combination of osteoconductivity and osteostimulation using β-CaSiO3/β-Ca3(PO4)2 composite bioceramics. Acta Biomater 2012;8(1):350–60.
[55] Kim MH, Choi MK. Effect of silicon supplementation in diets with different calcium levels on balance of calcium, silicon and magnesium, and bone status in growing female rats. Biol Trace Elem Res 2021;199(1):258–66.
[56] Casarrubios L, et al. Silicon substituted hydroxyapatite/VEGF scaffolds stimulate bone regeneration in osteoporotic sheep. Acta Biomater 2020;101:544–53.
[57] Kawanabe K, et al. Effects of injecting massive amounts of bioactive ceramics in mice. J Biomed Mater Res 1991;25(1):117–28.
[58] Kawanabe K, et al. Acute nephrotoxicity as an adverse effect after intraperitoneal injection of massive amounts of bioactive ceramic powders in mice and rats. J Biomed Mater Res 1992;26(2):209–19.
[59] Lai W, et al. Excretion of resorption products from bioactive glass implanted in rabbit muscle. J Biomed Mater Res 2005;75A(2):398–407.
[60] Lai W, Garino J, Ducheyne P. Silicon excretion from bioactive glass implanted in rabbit bone. Biomaterials 2002;23(1):213–7.
[61] Lin K, et al. Degradation and silicon excretion of the calcium silicate bioactive ceramics during bone regeneration using rabbit femur defect model. J Mater Sci Mater Med 2015;26(6):197.